Studying the role of ZnO nanostructure photoanodes for improving the photovoltaic performance of CdSe QDSSCs

M. Ramya[1,*] , T. K. Nideep[1], V. P. N. Nampoori[1], and M. Kailasnath[1]

[1] *International School of Photonics, Cochin University of Science and Technology, Kochi, India*

ABSTRACT

The photoanode is one of the principal components in QDSSCs and its organization has an incredible influence on the cell performance. Here we report the investigations on the influence of photoanode material based on ZnO nanodot, nanorod, nanoplate, and nanoflower on the performance of CdSe quantum dot-sensitized solar cells. For the QDSSCs fabrication, a well-dispersed aqueous solution of 5 nm sized CdSe quantum was synthesized using the chemical method, and the working electrode was dipped for 10 h for adsorption of photosensitizer on ZnO nanostructures. The performance of the photoanode is further improved by surface modification of quantum dot by the introduction of a ZnS buffer layer using the SILAR method. The ZnS buffer layer on the surface of the CdSe quantum dot decreases the backscattering of charge carriers. The optimized number of SILAR cycles for maximum device efficiency was estimated for each photoanode cells. The obtained efficiencies were found to increase from 0.50 to 0.92% (4th cycle), 1.55% (3rd cycle), 2.69% (3rd cycle), and 3.05% (2nd cycle) for the ZnO nanodot, nanorod, nanoplate, and nanoflower-based CdSe QDSSCs, respectively. Better conversion efficiency was noticed for cells fabricated with ZnO nanoflower as photoanode using a minimum number of SILAR cycles. Improved photon scattering, multiple reflections, light harvesting, and higher electron lifetime lead to the enhancement of device performance. The results give an insight into the efficiency improvement strategies for QDSSCs with ZnO nanostructure-based photoanode.

1 Introduction

Quantum dot-sensitized solar cells (QDSSCs) have been receiving great interest in the field of solar energy conservation due to the unique optical and chemical properties of inorganic quantum dots compared to organic dyes. Quantum dots exhibit many important physicochemical properties such as high absorption coefficient, tunability of bandgap, good photostability, large intrinsic dipole moment, and

Springer

tunable emission spectrum. More importantly, quantum dots generate multiple electron–hole pairs (MEG effect) leading to excellent theoretical photovoltaic device efficiency of 44% which is higher than the traditional Shockley and Queisser limit of $\sim 31\%$ [1–5]. However, the experimentally obtained power conversion efficiency of QDSSCs is considerably lower than the dye-sensitized solar cells (DSSCs). This scenario demands intensive research for the improvement of the photovoltaic performance of QDSSCs. The recent emerging trends in QDSSCs are shown in Fig. 1.

In quantum dots, the photocurrent generation is directly related to their size. With the change in size, the quantum dots can absorb different wavelength regions of the light and can attain higher theoretical efficiency. So far, researchers have developed different types of QDSSCs based on various semiconductor quantum dots such as CdSe, CdS, CdTe, PbS, PbSe, and InAs. Among these, Cadmium chalcogenides (CdTe, CdSe, and CdS) quantum dots are considered as a better choice in widespread research activities due to their distinct properties such as better stability in QDSSCs, effective photon absorption, size dependent bandgap tuning, multiple exciton generation, and ease of formation. Several reports show excellent size tunability of cadmium-based quantum dots and

their capability of converting visible light to electrical energy [2, 6–8]. We have reported the photovoltaic performance of QDSSCs fabricated using CdTe, CdS, and CdSe quantum dots as photosensitizers with TiO_2 as a working electrode [9]. The study showed an improved performance of CdSe-based QDSSCs compared to other cells due to their better absorption and lower effective mass of charge carriers. Hence, in the present work, we chose CdSe quantum dots as a photosensitizer for the fabrication of QDSSC. Various methods have been developed for improving the performance of QDSSCs viz. (1) Engineering the morphology of quantum dot surface, (2) QDSSCs composed of quantum dots with two or more sizes, (3) Coupling of different quantum dots in the form of core shells (4) Creation of a ZnS coating layer on the quantum dots to improve the photostability. In the present study, we choose the last method for improving the photovoltaic performance of the cell. The surface of the quantum dot was modified by coating the ZnS layer using Successive Ionic Layer Adsorption and Reaction (SILAR).

Apart from the use of quantum dots as a photosensitizer, the structural configuration of the photoanode also takes a critically important role in cell performance. The photoanode structure supports quantum dot loading, efficient charge transport,
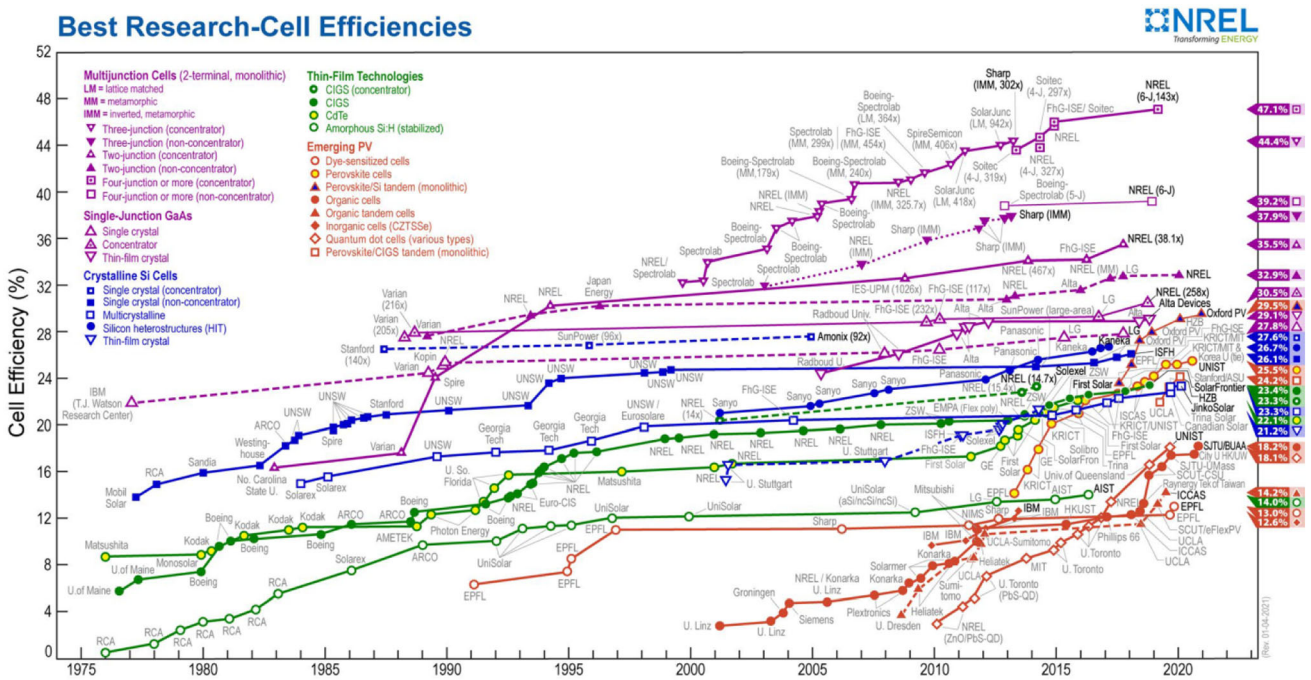

Fig. 1 NREL efficiency chart for photovoltaic technologies

quick electrolyte diffusion, and strong light scattering. Due to the large surface area and excellent electron transport, the mesoporous/heterogenous photoanode structure has been extensively studied both in DSSCs and QDSSCs. However, smaller-sized nanoparticles in the photoanode act as weak light scatterers. The weak scattering narrows down the distance traveled by the light within the photoanode and reduces the light absorption by the quantum dots. Therefore, higher dimensional structures are considered promising materials for photoanode [3, 6, 7]. There are many reports on the improvement of photovoltaic performance of QDSSCs based on different nanostructures of wide bandgap semiconductor oxides such as ZnO [2, 10], TiO_2 [6, 7], and SnO_2 [3, 11, 12]. Among these wide bandgap metal oxide semiconductors, TiO_2 is the one that has been most extensively used. In the case of TiO_2 nanoparticles, morphological engineering is a tedious process that involves high-temperature synthesis procedures. Hence, ZnO is a widely adopted alternative semiconductor material for TiO_2 which offers a similar wide direct bandgap and excellent electron mobility. Moreover, there exists a rich family of cost-effective, environment-friendly, and easily controllable diverse morphologies such as nanorods, nanotubes, nanosheets, nanoplates, nanocones, nanoflower, nanohelixes, nanosphere, nanorings[10, 13, 14]. The major drawbacks with the use of ZnO photoanode are the shallow light harvesting efficiency, low sensitizer loading, and low light scattering. By employing higher dimensional nano/microstructures we can effectively address these shortcomings. Here we report the fabrication of efficient CdSe QDSSCs by making use of different dimensional ZnO nanostructures as photoanode material.

2 Experimental

2.1 Preparation of working electrode

ZnO nanostructures were synthesized following the method described in our previous work [15]. In the synthesis procedure, 0.1 M Zinc acetate dihydrate and 0.5 M sodium hydroxide were dissolved in distinct solvents such as ethylene glycol, 1-butanol, acetic acid, and water, respectively. The precursor solutions were added dropwise under ultrasonication and were heated at a constant temperature 80 °C

for 2 h and sol was kept at rest for 1 day. As given in Fig. 2, the TEM images show that nanodot, nanorod, nanoplate, and nanoflower structures are formed while ethylene glycol,1-butanol, acetic acid, and water were used as solvents. The detailed morphological evolution, growth mechanism, and optical characterization were discussed in our published work [15]. In this work, we also discussed the photovoltaic performance of these structures in N719-based DSSCs. The results established the photoanode structural dependence of the cell performance giving rise to maximum efficiency of 4.1% for ZnO nanoflower-based DSSCs. This work motivated us to study the performance of QDSSCs when ZnO nanostructures are used as photoanode material. As the first step, we investigated the impact of different sized ZnO nanoparticles on the cell performance of N719 DSSCs and CdSe QDSSCs. It was found that the larger-sized ZnO nanoparticles show better device performance in both cases due to their higher Mie scattering. It was also found that the ZnS coating on the CdSe quantum dots can enhance QDSSCs performance [16].

The method of preparation of the working electrode is similar to our previous report [17]. ZnO paste was prepared by dissolving 100 mg of ZnO nanostructure powder in 3 ml of Triton X-100. The doctor blade technique was adopted for the preparation of thin film, and the resultant film was heated at 450 °C for 3 h.

### 2.2 Preparation of CdSe-sensitized ZnO photoanodes

The detailed synthesis procedure and characterization of the CdSe quantum dot were given in our previous publication [9]. Briefly, it involves the preparation of an aqueous solution of 2 g of $CdCl_2$, 6 g MSA, and 0.432 g Na_2SeO_3 and subsequent addition of 0.25 g of $NaBH_4$ solution into it. The pH was adjusted by addition of 1 M NaOH aqueous solution and the solution was heated at 70 °C for 1 h. We got well-dispersed CdSe quantum dots of size approximately 5 nm as shown in Fig. 3. The fabricated working electrode was dipped in quantum dot solution for 10 h to allow the adsorption of quantum dots over ZnO nanostructures by self-assembly.

Fig. 2 TEM image of synthesized ZnO nanostructures in various solvents [15]
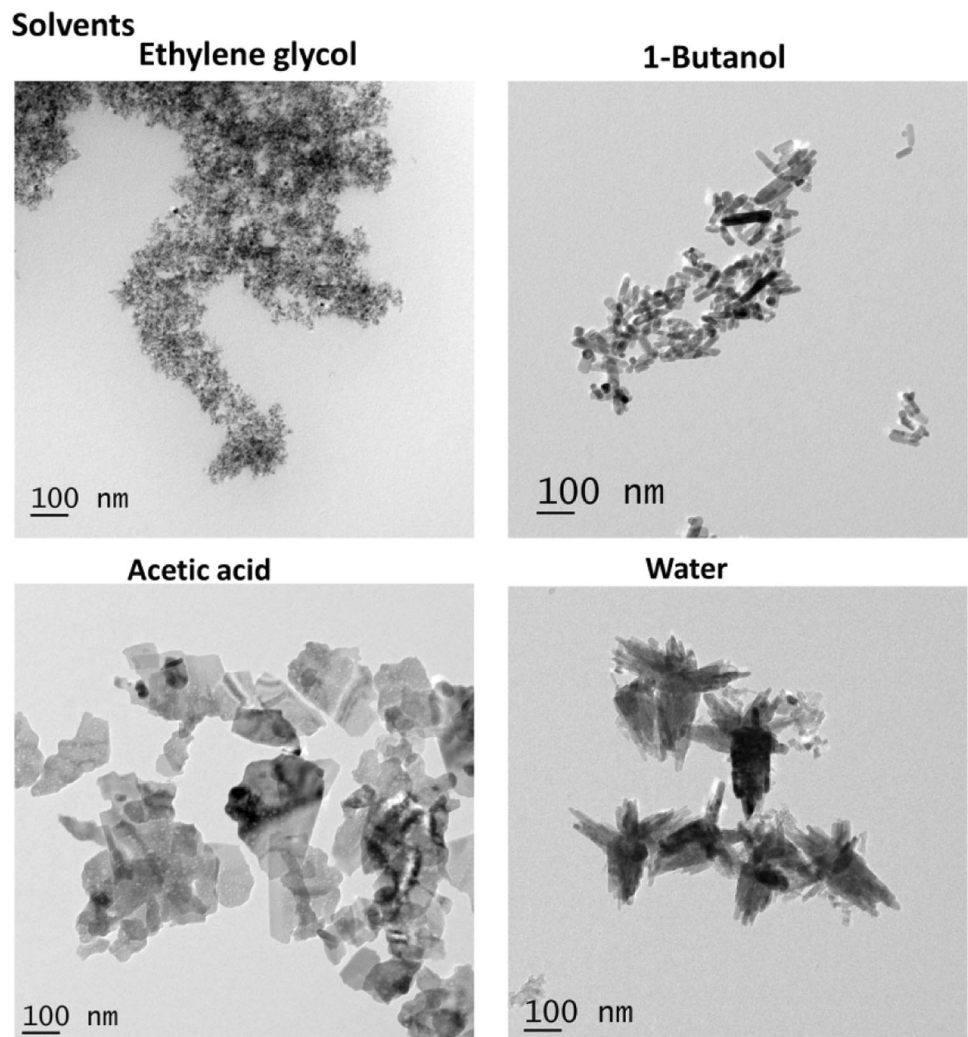
2.3 Formation of the ZnS layer

There are numerous reports on the ZnS coating on the quantum dots for enhancing the efficiency of the solar cell [2, 8, 18, 19]. We have fabricated and characterized QDSSCs with and without the ZnS layer. The ZnS passivation layer was coated by the SILAR cycle after the formation of CdSe quantum dots on ZnO. For this process, the synthesized photoanode was immersed in 0.1 M $ZnCl_2$ and Na_2S solutions alternately at a rate of 1 min/dip for each cycle. After each step of immersion, samples were rinsed with distilled water. This thin layer of ZnS on CdSe quantum dots reduces the surface recombination and improves cell performance. But, up to a certain limit, ZnS layer thickness affects cell performance due to the increase in the number of defects states in the lattice. So, the optimization of the ZnS layer thickness
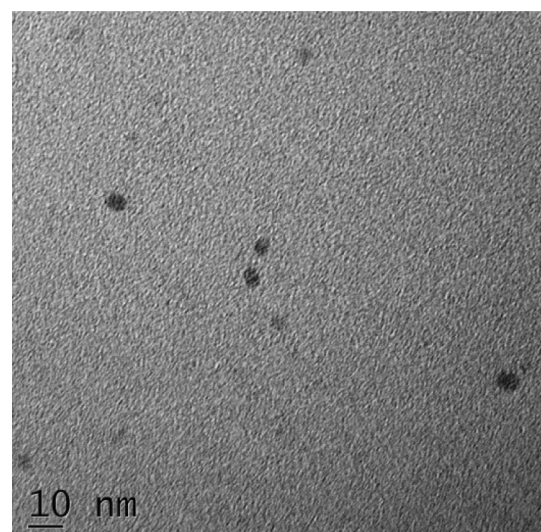
Fig. 3 TEM image of synthesized CdSe quantum dots [9]

is very important in this research. Hence, in this work, we have concentrated more on the number of SILAR cycles and their role in the device performance.

2.4 Fabrication and characterization of QDSSCs

The platinum counter electrode was prepared by coating a layer of platisol on the FTO glass plate. Finally, these two electrodes were sandwiched together and the electrolyte was injected. The schematic of the steps involved in the cell preparation is shown in Fig. 4.

The photovoltaic performance of the fabricated QDSSCs was analyzed using Keithely 2400 digital source meter and Newport solar simulator (AM 1.5G, 100mW/cm^2) as a light illuminator. IPCE was measured using PVE 300 photovoltaic QE system, and the lifetime was measured by CH electrochemical workstation.

3 Result and discussion

The synthesized nanostructures could strongly influence the energy conversion performance of QDSSCs in both the aspects of light harvesting and electron transport. Herein, four kinds of ZnO nanostructures, viz., nanodot, nanorod, nanoplate, and nanoflower are used as photoanode material in CdSe-based QDSSCs. Figure 5 shows the J–V curves for the QDSSCs based on these different photoanodes without ZnS treatment. The resulting photovoltaic parameters are depicted in Table 1. With J_{SC} = 1.67 mA/cm^2, V_{OC} = 0.60 V, and η = 0.50% the fabricated cells with the ZnO nanoflower photoanode show better performance compared to other cells. The nanoplate-based cell showed the second highest efficiency of 0.22%. The QDSSCs based on other structures showed negligible efficiency.

There were noticeable differences in current density (J_{SC}) values of the devices, which mainly depend on the light harvesting ability of the photoanode. The photon capturing ability of the photosensitizer can be enhanced by improving the light scattering inside the device. Experimental results suggest that excellent photo scattering ability and relatively high surface area of photoanode structure leads to the highest J_{SC} and η values in both DSSCs and QDSSCs

[3, 6, 7, 10, 6, 7, 6, 7]. In agreement with this, the nanoflower-based photoanode offers the best photovoltaic performance. The higher reflectivity of ZnO nanoflowers leads to better photon scattering property compared to other structures shown in Fig. 6. Another important parameter is the surface area of the synthesized nanostructures which affects the quantum dot adsorption capacity. The surface area of synthesized ZnO nanostructures was measured using BET analysis (Tristar 3020). The estimated surface area is 19.26, 27.67, 40.91, and 60.39 m^2/g for ZnO nanodot, nanorod, nanoplate, and nanoflower, respectively. ZnO nanoflower sample has a higher surface area compared to other structures. Hence, more CdSe quantum dots are adsorbed on the surface of the photoanode fabricated using these nanoflower powdered samples. The higher surface area, random orientation, and higher photon scattering provide better conversion efficiency for the nanoflower CdSe QDSSCs. The next highest efficiency was obtained for ZnO nanoplate-based cells due to its second highest surface area and reflectivity. The other two structures; nanodots and nanorods have lower reflectivity and surface area, which was reflected in their photoconversion efficiencies. For further improvement in photovoltaic performance, the photoanode was treated with ZnS using the SILAR method.

After ZnS treatment, both J_{SC} and V_{OC} values are found to be improved, and an increase in efficiency was also observed. ZnS layer creates quantum confinement of charge carriers, which improves the cell performance. Here, the ZnS layer was coated over CdSe quantum dots using 5 SILAR cycles. The results showed that the efficiency increases with the number of SILAR up to a certain limit. Beyond that limit, the performance was dropped off. The ZnS layer blocks the backward electron flow and limits the leakage of the electron into the electrolyte, thereby increasing the fill factor and efficiency of the cells. But as the ZnS layer thickness increases, larger numbers of defect states are generated causing the efficiency to decrease drastically. The detailed mechanism of the action of the ZnS buffer layer is explained in our previous reports [8, 9, 16]. Figure 7 and Table 2 show the cell performance of ZnS treated QDSSCs using ZnO nanodots as a photoanode. Here we could observe an improvement in the cell parameters such as V_{OC}, J_{SC}, FF, and η with the ZnS treatment. It also shows that the obtained maximum efficiency was 0.92% corresponding to the 4th SILAR cycle. After the 4th cycle, a
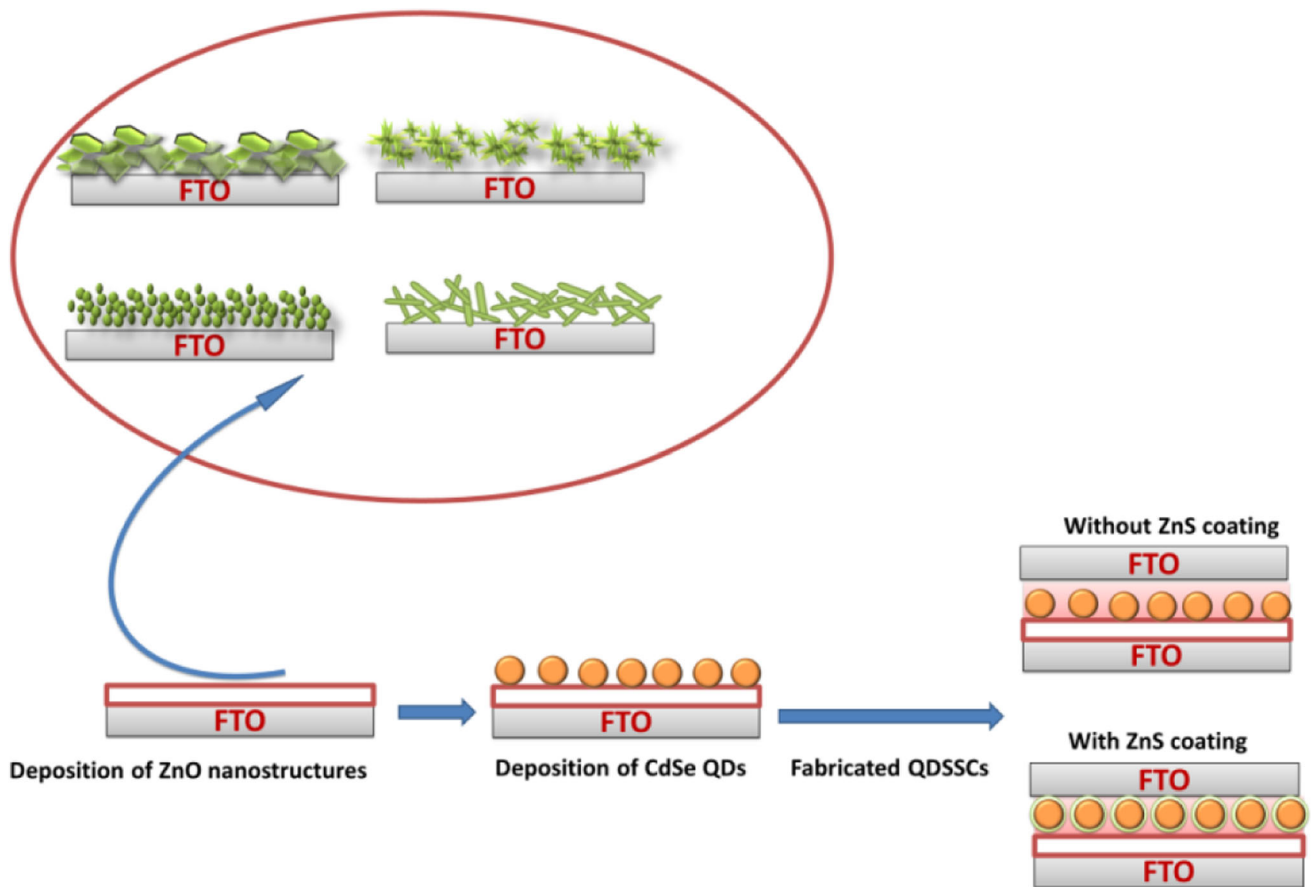
Fig. 4 Schematic representation of CdSe QDSSCs fabrication with and without ZnS coating
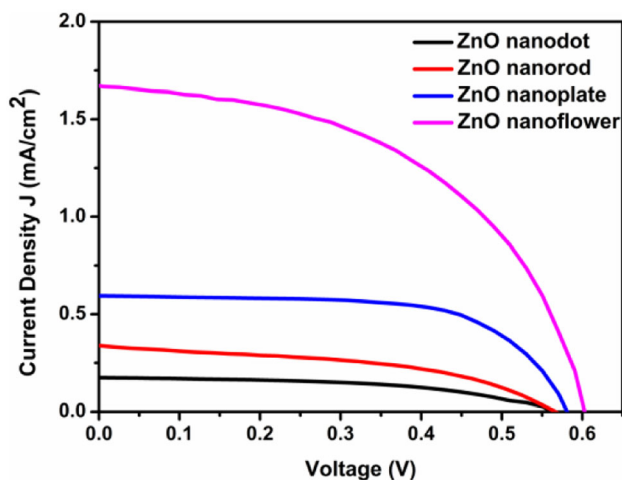
Fig. 5 *J–V* characteristics of fabricated CdSe QDSSCs without the ZnS coating using ZnO nanostructures as a photoanode

drop in efficiency was noticed. Hence, the 4th cycle is the optimum cycle in the case of the ZnO nanodot CdSe QDSSCs.

Table 1 Photovoltaic parameters of fabricated CdSe QDSSCs without ZnS coating using ZnO nanostructures as a photoanode

ZnO nanostructures	J_{SC} (mA/cm^2)	V_{OC} (V)	FF	η(%)
Dot	0.17	0.562	0.412	0.005
Rod	0.34	0.566	0.476	0.094
Plate	0.59	0.579	0.502	0.219
flower	1.67	0.60	0.522	0.502

In the case of QDSSCs fabricated using ZnO nanorod and nanoplate, the optimum number of SILAR cycles used for the maximum efficiency was 3. The obtained maximum photoconversion efficiency was 1.55% for nanorod and 2.69% for nanoplate photoanode-based cells. The *J–V* curve for the fabricated QDSSCs using ZnO nanorods and nanoplates-based photoanodes are shown in Figs. 8 and 9, respectively, and the estimated photovoltaic parameters are depicted in Tables 3 and 4.
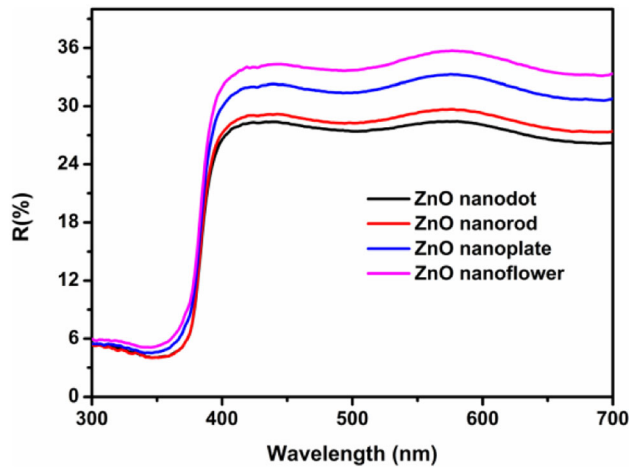
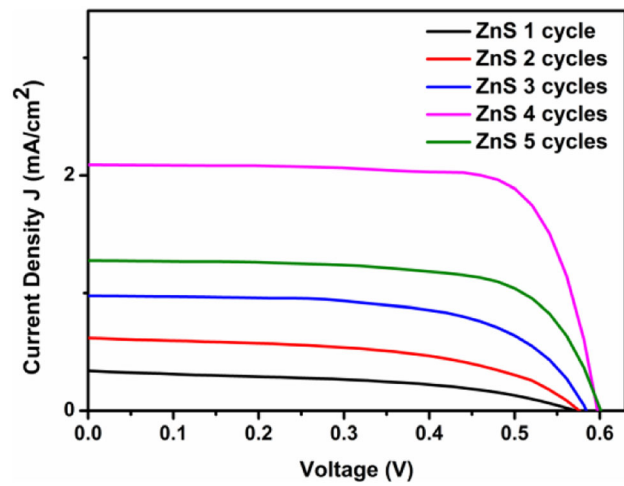**Fig. 6** Reflection spectra of ZnO nanostructure films [15]

Fig. 7 *J–V* characteristics of fabricated CdSe QDSSCs with ZnS coating using ZnO nanodot as a photoanode

Table 2 Photovoltaic parameters of fabricated CdSe QDSSCs with ZnS coating using ZnO nanodot as a photoanode

No. of SILAR	J_{SC} (mA/cm^2)	V_{OC} (V)	FF	η(%)
1	0.336	0.573	0.461	0.089
2	0.619	0.576	0.523	0.186
3	0.977	0.584	0.607	0.346
4	2.083	0.597	0.642	0.920
5	1.389	0.599	0.634	0.529

In the case of ZnO nanoflower photoanode QDSSCs, the number of SILAR cycles for maximum cell efficiency of 3.05% was found to be reduced to 2. The obtained efficiency is higher than the other cells composed of ZnO nanodot, nanorod, and nanoplate.

Here also larger surface area and random orientation of nanoflower offer an increased quantum dot loading and strong Mie scattering. The larger quantum dot loading permits higher light harvesting ability and J_{SC} value. The prominent light scattering effect could induce multiple reflections in the visible region and improvement in the visible light absorption. The *J–V* curve and a summary of the photovoltaic parameters are shown in Fig. 10 and Table 5.

Figure 11 shows the Incident Photon-to-Current Conservation efficiency (IPCE) spectra of the fabricated cells with optimum SILAR cycles. The cell with ZnO nanoflower photoanode exhibits a higher peak value of IPCE occurring at 460 nm compared with the other cells. This spectrum also indicates the higher light harvesting ability of the nanoflower photoanode QDSSC device, which is in agreement with the highest observed value of the photocurrent. The efficiency of the device is found to increase with a reduction in the interface charge recombination which results in a large electron lifetime. The electron lifetime of the fabricated devices was calculated using Bode-Phase plot [9] ($\tau_e = \frac{1}{2\pi f_{max}}$) shown in Fig. 12. The tabulated electron lifetimes are 2.59, 4.29, 47 and 178 ms for devices fabricated using ZnO nanodot, rod, plate, and flower, respectively. Since the increase in electron lifetime causes an improved photovoltaic performance of QDSSCs. Table 6 shows the summarized parameters of fabricated cells with maximum obtained efficiency. The larger surface area of the nanoflower structure increases the QDs loading and the lifetime leading to a reduction in the
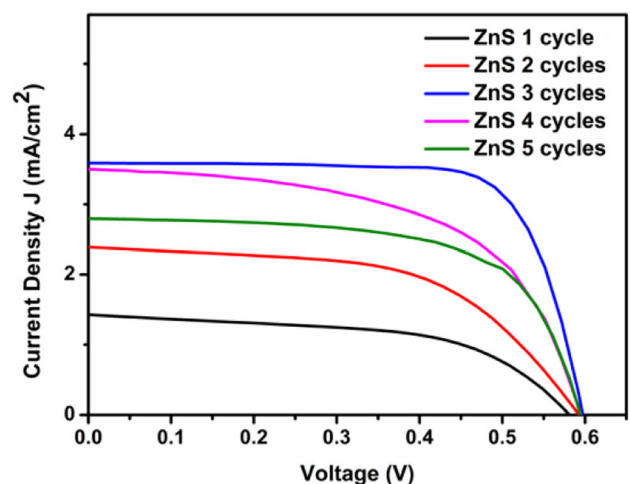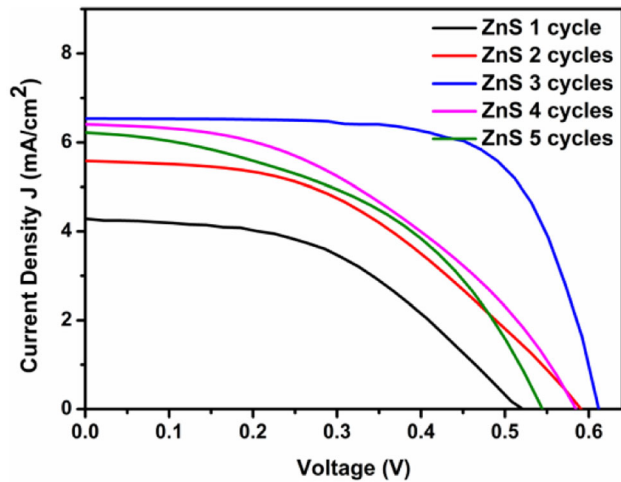

Fig. 8 *J–V* characteristics of fabricated CdSe QDSSCs with ZnS coating using ZnO nanorod as a photoanode

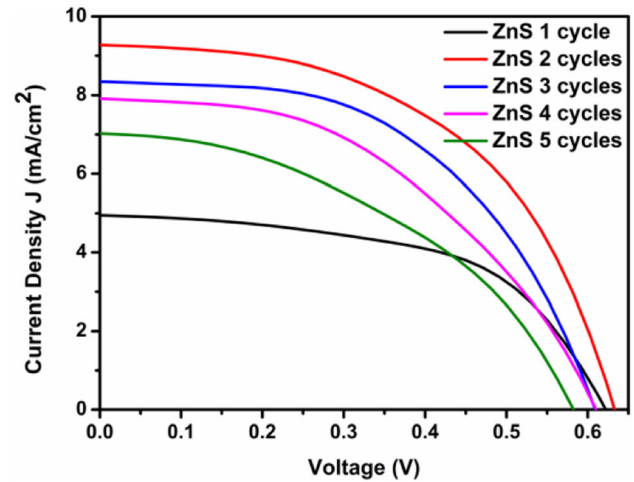**Fig. 9** *J–V* characteristics of fabricated CdSe QDSSCs with a ZnS coating using ZnO nanoplate as a photoanode

Table 3 Photovoltaic parameters of fabricated CdSe QDSSCs with ZnS coating using ZnO nanorod as a photoanode

No. of SILAR	J_{SC} (mA/cm^2)	V_{OC} (V)	FF	η(%)
1	1.427	0.579	0.546	0.464
2	2.391	0.591	0.551	0.772
3	3.584	0.597	0.726	1.554
4	3.517	0.598	0.587	1.236
5	2.790	0.596	0.573	1.046

Table 4 Photovoltaic parameters of fabricated CdSe QDSSCs with ZnS coating using ZnO nanoplate as a photoanode

| No. of SILAR	J_{SC} (mA/cm^2)	V_{OC} (V)	FF	η(%)
1	1.409	0.581	0.553	0.454
2	5.571	0.590	0.587	1.425
3	6.535	0.612	0.673	2.690
4	6.405	0.582	0.621	1.619
5	6.235	0.544	0.592	1.569

recombination rate. Also, the higher IPCE and scattering ability helps to enhance the efficiency of cells fabricated using ZnO nanoflower. The next highest efficiency was obtained for ZnO nanoplate-based cells because of its second highest photovoltaic parameters, including J_{SC}, IPCE, lifetime, surface area, and reflectivity. The other structures showed lower values of efficiency due to their smaller photovoltaic parameters.

Fig. 10 *J–V* characteristics of fabricated CdSe QDSSCs with a ZnS coating using ZnO nanoflower as a photoanode

Table 5 Photovoltaic parameters of fabricated CdSe QDSSCs with ZnS coating using ZnO nanoflower as a photoanode

No. of SILAR	J_{SC} (mA/cm^2)	V_{OC} (V)	FF	η(%)
1	4.951	0.623	0.681	1.707
2	9.281	0.633	0.742	3.053
3	8.342	0.606	0.632	2.359
4	7.874	0.607	0.615	2.186
5	4.075	0.581	0.554	1.756
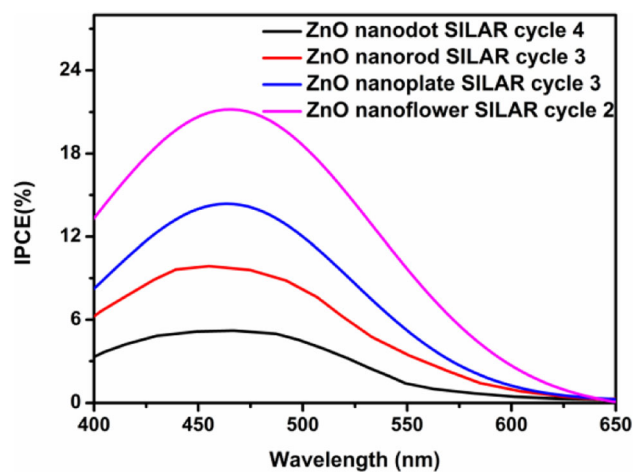
Fig. 11 IPCE spectra of CdSe-sensitized solar cell with optimum ZnS coating using ZnO nanostructures as photoanode

In one of our recently reported works [9], CdSe QDSSCs were fabricated using TiO$_2$ nanoparticles as photoanode to get maximum efficiency of 1.98%. In the present work, CdSe QDSSCs fabricated using

ZnO plate and nanoflowers as photoanode materials show higher efficiency (2.69% and 3.05%) than TiO₂-based cells. Also, the obtained efficiency is found to be larger compared with the previously published reports [6, 21, 27–37]. Hence, N719-based DSSCs [15] and CdSe-based QDSSCs were fabricated using these ZnO nanostructures. In both cases, we could achieve better power conversion efficiency. The results suggest that the synthesized ZnO nanostructures are excellent photoanode materials for solar cell fabrication. For further improvement in the photovoltaic performance, two modifications to the photoanode material are proposed. The first one is to synthesize ZnO higher dimensional microstructures with better crystallinity and the second one is the creation of an additional scattering layer on the surface of ZnO nanostructures to increase the scattering ability of the photoanode. The works along these lines are in progress in our lab.

4 Conclusion

In conclusion, we have developed a better ZnO-based photoanode material for QDSSCs fabrication. In the present study, these prepared ZnO nanostructures were used as a photoanode material for the fabrication of CdSe-based QDSSCs. The device performance of the fabricated cells was found to vary according to the structural changes in the photoanode material. Also, the ZnS treatment effectively improved the performance of QDSSCs. By this treatment, the enhancement in power conversion efficiency was found to vary from 0.5% to 0.92%, 1.55%, 2.69%, and 3.05% respectively for the dot, rod, plate, and flower-based QDSSCs. The ZnS layer was found to reduce the backward electron scattering and prevent the electron trapping. Compared to the cells based on other structures, nanoflower-based CdSe QDSSCs showed the highest power conversion efficiency due to enhanced quantum dot adsorption, photon scattering, multiple reflections, and the inhibition of charge carrier recombination. The results indicate that the low-temperature structural tunability of ZnO nanoparticles can be potentially applied to solar cell fabrication as it remains to be a better alternative to TiO₂ photoanode.
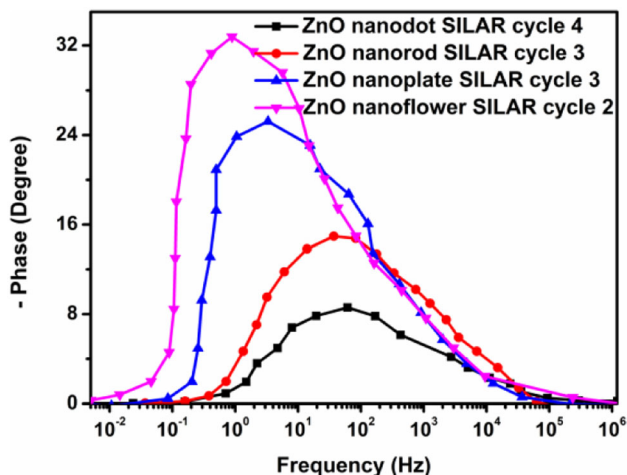
Fig. 12 Bode-Phase plot of CdSe QDSSCs with optimum ZnS layer using ZnO nanostructures as photoanode

Table 6 Photovoltaic parameters of CdSe QDSSCs with ZnS coating using ZnO nanostructures as a photoanode

ZnO nanostructure	Optimum SILAR cycles	BET surface area(m²/g)	τ_e (ms)	η (%)
Nanodot	4	19.26	2.59	0.920
Nanorod	3	27.67	4.29	1.554
Nanoplate	3	40.91	47	2.690
Nanoflower	2	60.39	178	3.053

Acknowledgements

References

1. H. Goodwin, T.C. Jellicoe, N.J.L.K. Davis, M.L. Böhm, Multiple exciton generation in quantum dot-based solar cells. Nanophotonics **7**, 111–126 (2018)

2. M. Ganjian, M. Kolahdouz, A. Aletayeb, M. Norouzi, ZnS shell-like CdS quantum dot-sensitized solar cell grown by SILAR approach; effect of electrolyte, counter electrode, and shell thickness. Vaccum **146**, 548–553 (2017)

3. Y. Rui et al., Liquid-liquid interface assisted synthesis of SnO$_2$ nanorods with tunable length for enhanced performance in dye-sensitized solar cells. Electrochim. Acta **227**, 49–60 (2017)

4. V. Kalarivalappil, S.J. Hinder, S.C. Pillai, V. Kumar, Stability studies of CdS sensitized TiO$_2$ nanotubes prepared using the SILAR method. J. Environ. Chem. Eng. **6**, 1404–1413 (2018)

5. H.K. Jun, M.A. Careem, A.K. Arof, Quantum dot-sensitized solar cells—perspective and recent developments: a review of Cd chalcogenide quantum dots as sensitizers. Renew. Sustain. Energy Rev. **22**, 148–167 (2013)

6. C. Chen et al., Ultralong rutile TiO$_2$ nanorod arrays with large surface area for CdS/CdSe quantum dot-sensitized solar cells. Electrochim. Acta **121**, 175–182 (2014)

7. R. Zhou et al., Photoanodes with mesoporous TiO$_2$ beads and nanoparticles for enhanced performance of CdS/CdSe quantum dot co-sensitized solar cells. Electrochim. Acta **135**, 284–292 (2014)

8. T.K. Nideep, M. Ramya, M. Kailasnath, The influence of ZnS buffer layer on the size dependent efficiency of CdTe quantum dot sensitized solar cell. Superlattices Microstruct. **130**, 175–181 (2019)

9. T.K. Nideep, M. Ramya, M. Kailasnath, An investigation on the photovoltaic performance of quantum dot solar cells sensitized by CdTe, CdSe and CdS having comparable size. Superlattices Microstruct. **141**, 106477 (2020)

10. D. Wu et al., ZnO nanorods with tunable aspect ratios deriving from oriented-attachment for enhanced performance in quantum-dot sensitized solar cells. Electrochim. Acta **231**, 1–12 (2017)

11. A. Hossain, G. Yang, M. Parameswaran, J.R. Jennings, Q. Wang, Mesoporous SnO$_2$ spheres synthesized by electrochemical anodization and their application in CdSe-sensitized solar cells. J. Phys. Chem. C **114**, 21878–21884 (2010)

12. S. Pan et al., Hierarchical SnO$_2$ hollow sub-microspheres for panchromatic PbS quantum dot-sensitized solar cells. J. Alloys Compd. **709**, 187–196 (2017)

13. J. Cai et al., Electrochimica Acta A novel hierarchical ZnO-nanosheet-nanorod-structured film for quantum-dot-sensitized solar cells. Electrochim. Acta **274**, 326–333 (2018)

14. S. Anas et al., Engineered hetero structured arrays of ZnO NanoX (X = discs, rods and wires) and CdTe quantum dots for advanced electron transport applications. Mater. Des. **141**, 267–275 (2018)

15. M. Ramya, T.K. Nideep, V.P.N. Nampoori, M. Kailasnath, Solvent assisted evolution and growth mechanism of zero to three dimensional ZnO nanostructures for dye sensitized solar cell applications. Sci. Rep. **11**, 1–14 (2021)

16. M. Ramya, T.K. Nideep, V.P.N. Nampoori, M. Kailasnath, The impact of ZnO nanoparticle size on the performance of photoanodes in DSSC and QDSSC: a comparative study. J. Mater. Sci. Mater. Electron. (2020). https://doi.org/10.1007/s10854-020-05065-0

17. M. Ramya, T.K. Nideep, V.P.N. Nampoori, M. Kailasnath, Understanding the role of alcohols in the growth behaviour of ZnO nanostructures prepared by solution based synthesis and their application in solar cells. New J. Chem. **43**, 17980–17990 (2019)

18. C. Liu, L. Mu, J. Jia, X. Zhou, Y. Lin, Boosting the cell efficiency of CdSe quantum dot sensitized solar cell via a modified ZnS post-treatment. Electrochim. Acta **111**, 179–184 (2013)

19. N. Guijarro, J.M. Campina, Q. Shen, T. Toyoda, T. Lana-Villarreal, R. Gómez, Uncovering the role of the ZnS treatment in the performance of quantum dot sensitized solar cells. Phys. Chem. Chem. Phys. **13**, 12024–12032 (2011)

20. N. Singh, Z. Salam, A. Subasri, N. Sivasankar, A. Subramania, Development of porous TiO$_2$ nano fibers by solvosonication process for high performance quantum dot sensitized solar cell. Sol. Energy Mater. Sol. Cells **179**, 417–426 (2018)

21. C. Zhou et al., Chemistry one-pot synthesis of CdSe @ CdS core @ shell quantum dots and their photovoltaics application in quantum-dot-sensitized ZnO nanorods. J. Photochem. Photobiol. A Chem. **332**, 251–257 (2017)

22. T. Majumder, S. Dhar, P. Chakraborty, K. Debnath, Advantages of ZnO nanotaper photoanodes in photoelectrochemical cells and graphene quantum dot sensitized solar cell applications. J. Electroanal. Chem. **813**, 92–101 (2018)

23. S.S. Mali, H. Kim, C.S. Shim, P.S. Patil, J.H. Kim, C.K. Hong, Surfactant free most probable TiO_2 nanostructures via hydrothermal and its dye sensitized solar cell properties. Sci. Rep. **3**, 1–8 (2013)

24. H. Lu, W. Tian, J. Guo, L. Li, Interface engineering through atomic layer deposition towards highly improved performance of dye-sensitized solar cells. Sci. Rep. **5**, 1–12 (2015)

25. Z. Li et al., Mesoporous TiO_2 yolk-shell microspheres for dye-sensitized solar cells with a high efficiency exceeding 11 %. Sci. Rep. **5**, 1–8 (2015)

26. X. Ren, L. Yu, Z. Li, H. Song, Q. Wang, The influence of CdS intermediate layer on CdSe/CdS co-sensitized free-standing TiO_2 nanotube solar cells. Superlattices Microstruct. **113**, 696–705 (2018)

27. D. Trans, R.S. Devan, Y. Ma, P.S. Patil, PbS quantum dot sensitized anatase TiO_2 nanocorals for quantum dot-sensitized solar cell applications. Dalt. Trans. **41**, 6130–6136 (2012)

28. Y. Zhang, J. Tian, K. Jiang, J. Huang, L. Zhang, A novel method for fabrication of CdS quantum dot-sensitized solar cells. J. Mater. Sci. Mater. Electron. **28**, 14103–14109 (2017)

29. Z. Mo et al., Growth of ZnO nanowires and their applications for CdS quantum dots sensitized solar cells. Opt. Int. J. Light Electron Opt. **149**, 63–68 (2017)

30. M. Abdul, M. Awais, E. Sun, J. Ho, T. Joo, Improved light absorbance and quantum-dot loading by macroporous TiO_2 photoanode for PbS quantum-dot-sensitized solar cells. Mater. Chem. Phys. **196**, 170–176 (2017)

31. P. Lekha, A. Balakrishnan, K.R.V. Subramanian, S.V. Nair, Size dependent electron transfer from CdTe quantum dots linked to TiO_2 thin films in quantum dot sensitized solar cells. Mater. Chem. Phys. **141**, 216–222 (2013)

32. K. Meng, P.K. Surolia, O. Byrne, K.R. Thampi, Efficient CdS quantum dot sensitized solar cells made using novel Cu_2S counter electrode. J. Power Sources **248**, 218–223 (2014)

33. K. Surana, I.T. Salisu, R.M. Mehra, B. Bhattacharya, A simple synthesis route of low temperature CdSe–CdS core-shell quantum dots and its application in solar cell. Opt. Mater. (Amst) **82**, 135–140 (2018)

34. S.K. Kokate, A.T. Supekar, P.K. Baviskar, B.M. Palve, CdS sensitized pristine and Cd doped ZnO solar cells: effect of SILAR cycles on optical properties and efficiency. Mater. Sci. Semicond. Process. **80**, 179–183 (2018)

35. Y. Zhang et al., TiO_2 nanorod arrays/ZnO nanosheets heterostructured photoanode for quantum-dot-sensitized solar cells. Sol. Energy **166**, 371–378 (2018)

36. A. Arivarasan, S. Bharathi, V.V. Ganapathy, S. Ramasamy, Evaluation of reaction parameters dependent optical properties and its photovoltaics performances of CdTe QDs. J. Inorg. Organomet. Polym. Mater. **28**, 1263–1275 (2018)

37. A. Badawi, N. Al-hosiny, S. Abdallah, S. Negm, H. Talaat, Tuning photocurrent response through size control of CdTe quantum dots sensitized solar cells. Sol. Energy **88**, 137–143 (2013)